Aging phenomena in poly(methyl methacrylate) thin films: Memory and rejuvenation effects

K. Fukao* and A. Sakamoto†
Department of Polymer Science, Kyoto Institute of Technology, Matsugasaki, Kyoto 606-8585, Japan
(Received 23 October 2004; published 21 April 2005)

The aging dynamics in thin films of poly(methyl methacrylate) (PMMA) have been investigated through dielectric measurements for different types of aging processes. The dielectric constant was found to decrease with increasing aging time at an aging temperature in many cases. An increase in the dielectric constant was also observed in the long-time region ($\geqslant$11 h) near the glass transition temperature for thin films with thickness less than 26 nm. In the constant-rate mode including a temporary stop at a temperature T_a, the memory of the aging at T_a was found to be kept and then to be recalled during the subsequent heating process. In the negative-temperature cycling process, a strong rejuvenation effect has been observed after a temperature shift from the initial temperature T_1 to the second temperature T_2 ($=T_1+\Delta T$) when $\Delta T \approx -20$ K. Furthermore, a full memory effect has also been observed for the temperature shift from T_2 to T_1. This suggests that the aging at T_1 is totally independent of that at T_2 for $\Delta T \approx -20$ K. As $|\Delta T|$ decreases, the independence of the aging between the two temperatures was found to be weakened—i.e., the effective time, which is a measure of the contribution of the aging at T_1 to that at T_2, is a decreasing function of $|\Delta T|$ in the negative region of ΔT. As the film thickness decreases from 514 nm to 26 nm, the $|\Delta T|$ dependence of the effective time was found to become much stronger. The contribution of the aging at T_2 to that at T_1 disappears more rapidly with increasing $|\Delta T|$ in thin-film geometry than in the bulk state.

DOI: 10.1103/PhysRevE.71.041803 PACS number(s): 36.20.−r, 71.55.Jv, 81.05.Lg, 77.22.Ch

I. INTRODUCTION

In glassy materials it is well known that a very slow relaxation towards an equilibrium state is observed below the glass transition temperature T_g [1,2]. This slow relaxation is called aging and is regarded as an important common property characteristic of disordered materials such as spin glasses [3–6], orientational glasses [7], supercooled liquids [8], relaxor ferroelectrics [9], and polymer glasses [10,11]. Investigations of such disordered systems revealed that *memory and rejuvenation* effects are observed during the aging process. The characteristic behavior of the aging dynamics below T_g is closely related to the nature of the glass transition. Therefore, it is expected that elucidation of the aging phenomena can lead to a full understanding of the mechanism of the glass transition in disordered materials, which is still a controversial topic [12].

In polymeric systems, Kovacs *et al.* investigated the memory effects observed in aging phenomena [13]. In their experiments, a volume relaxation was measured on a glassy state located on a line extrapolated from the equilibrium line corresponding to a liquid state. Because the glassy state is on the equilibrium line, it is expected that no further volume change occurs in this state. However, their results suggest that the volume relaxation strongly depends on the thermal history which the polymer had experienced before arriving at this equilibrium state. In other words, the thermal history can be memorized within the glassy state of polymers. Recent experiments by Miyamoto *et al.* revealed that polymeric materials can keep not only thermal history but also mechanical history in their glassy states and the histories can be recalled upon the glass transition, through measurements of tension in rubbers [14].

In spin glasses, interesting studies of aging phenomena have been done in recent years [3–5]. In experiments on the $CdCr_{1.7}In_{0.3}S_4$ insulating spin glass, a relaxation of the imaginary part of the magnetic ac susceptibility χ'' was observed in a temperature cycling. First, the sample is cooled down to a temperature T_1 below T_g and is kept at this temperature for a period of τ_1. Then the temperature is changed from T_1 to $T_1+\Delta T$ ($\Delta T<0$) and kept for τ_2, and after that the temperature is returned to T_1. It was observed that upon cooling from T_1 to $T_1+\Delta T$, the system *rejuvenates* and returns to a zero-age structure even after a long stay at the higher temperature T_1. The interesting point is that the system has a *perfect memory* of the past thermal history; i.e., when heated back to T_1, the susceptibility χ'' agrees well with the value that χ'' had reached just at the end of the first stage of the aging at T_1. As for polymeric systems, a similar measurement on the aging dynamics has been done for the dielectric constant in poly(methyl methacrylate) (PMMA) by Bellon *et al.* to investigate the memory effects of the aging dynamics. Although a memory effect similar to that in spin glasses has been observed also in PMMA in their studies [10,11], more detailed investigations would be required to extract a universal behavior of the aging dynamics in polymer glasses and to compare the aging dynamics between polymeric systems and spin glasses.

It is very natural to believe that the aging dynamics in the glassy state mentioned above are related to the nature of the glass transition. Recent investigations of the glass transition in thin-film geometry show that there is a strong dependence

*Corresponding author. Electronic address: fukao@kit.ac.jp
†Present address: Department of Macromolecular Science, Graduate School of Science, Osaka University, Toyonaka, Osaka 560-0043, Japan.

of the glass transition temperature and the dynamics on the film thickness and system size [15,16,19]. Therefore, it is expected that the aging dynamics depend on the film thickness [20], and through such investigations it would be possible to approach the basic mechanism of the glass transition. From the technical point of view, thin-film geometry is ideal for dielectric measurements because the smaller thickness of the films enhances the resolution of the capacitance measurements. For this reason, precise measurements can be done for thin-film geometry.

In this study, we measured the time evolution of the complex electric capacitance of PMMA films during the aging process using dielectric relaxation spectroscopy. The purpose of this study is to investigate the relaxation dynamics of nonequilibrium states including memory and rejuvenation effects in polymeric systems and to elucidate the thickness dependence of the aging dynamics.

This paper consists of six sections. After giving experimental details in Sec. II, the aging dynamics at a given temperature are shown in Sec. III. In Sec. IV, experimental results on memory and rejuvenation effects are presented for two different thermal histories. After discussing the experimental results in Sec. V, a summary of this paper is given in Sec. VI.

II. EXPERIMENT

Polymer samples used in this study are atactic PMMA purchased from Scientific Polymer Products, Inc. The weight-averaged molecular weight $M_w = 3.56 \times 10^5$ and $M_w/M_n = 1.07$, where M_n is the number-averaged molecular weight. The glass transition temperature T_g determined by differential scanning calorimetry (DSC) is about 380 K for the bulk samples of PMMA used in this study. The value of T_g in thin films with $d = 26$ nm is lower by 7 K than T_g in the bulk samples. Thin films are prepared on aluminum-vacuum-deposited glass substrate using a spin-coat method from a toluene solution of PMMA. The thickness of the films is controlled to be 20–514 nm by changing the concentration of the solution of PMMA. The thickness is evaluated from the value of the electric capacitance at 273 K of as-prepared films before measurements in the same way as in previous papers [16–18]. After annealing at 343 K, aluminum is vacuum deposited again to serve as upper electrodes. A copper wire is attached to the end of the electrode with conducting paste so that the polymer samples can easily be connected with the measurement system. The sample prepared in the above way is mounted inside a sample cell. The temperature of the sample cell is controlled through a heater wound around the cell using a temperature controller. The temperature of the polymer sample is monitored as the temperature measured through a thermocouple put onto the back side of the glass substrate. Heating above 400 K was done several times before the measurements so that the contact between the polymer films and the substrate is stabilized. The temperature of the sample is stabilized within 2 min after a temperature jump. The stability of the temperature control is ±0.1 K.

Dielectric measurements were done by an *LCR* meter (HP4284A). The frequency range of the applied electric field was from 20 Hz to 1 MHz. The voltage level was controlled so that the strength of the applied electric field remains almost constant independent of the film thickness. The typical electric field was 2×10^6 V/m. In our measurements, the complex electric capacitance of the sample condenser $C^*(T)$ was measured and then converted into the dynamic (complex) dielectric constant $\epsilon^*(T)$ by dividing the $C^*(T)$ by the geometrical capacitance $C_0(T_0)$ at a standard temperature T_0. The value of C^* is given by $C^* = \epsilon^* \epsilon_0 S/d$ and $C_0 = \epsilon_0 S/d$, where ϵ_0 is the permittivity in vacuum, S is the area of the electrode, and d is the film thickness. For evaluation of ϵ^* and C_0, we use the thickness d which is determined at $T_0 = 273$ K and $S = 8 \times 10^{-6}$ mm^2. Because ϵ^* and C^* are complex numbers, we define the real and imaginary parts as follows: $\epsilon^* = \epsilon' - i\epsilon''$ and $C^* = C' - iC''$.

III. AGING DYNAMICS

In this section, we show the relaxation behavior during the isothermal aging process at a given temperature T_a. In order to remove the thermal history of the sample, the system is heated up to 403 K ($>T_g$) and is kept at 403 K for a couple of hours. After this procedure the system is cooled down to T_a at the rate of 0.5 K/min and the measurement of the complex electric capacitance is started. Figure 1(a) displays the time evolution of the imaginary component of the dynamic dielectric constant ϵ'' at various aging temperatures for thin films with thickness of 20 nm. In Fig. 1(a), it is found that ϵ'' is a monotonically decreasing function of the aging time t_w. The vertical axis in this figure is the value of ϵ'' normalized with respect to the initial value $\epsilon''(0)$. The origin of the time axis is defined as the time at which the temperature of the system reached T_a. The decrease in the dielectric constant corresponds to the smaller response against an applied external field, and hence this indicates that the system goes down to a deeper valley of the free energy via thermal activations within the energy landscape picture [21,22]. In other words, the system approaches an equilibrium state as the time t_w elapses at a temperature T_a below T_g. The aging phenomena can be interpreted as this approach to the equilibrium state.

In an equilibrium state, the dielectric constant can be uniquely specified as functions of temperature T, pressure p, and the frequency of the applied electric field f for the polymer films with a fixed thickness. For simplicity, we ignore the effect of the pressure in the discussions below. If the system is in a nonequilibrium state, it is not easy to specify the dielectric constant, and the aging phenomena must be taken into account. The dielectric constant depends on the thermal history that the sample has experienced. In general, if the system is aged at a temperature $T_{a,1}$ for a period of $t_{w,1}$, at $T_{a,2}$ for $t_{w,2}$,..., and at $T_{a,n}$ for $t_{w,n}$, the dielectric loss ϵ'' can be specified by the following description:

$$\epsilon'' = \epsilon''(T, \omega; \{t_{w,j}(T_{a,j})\}), \tag{1}$$

where $\omega = 2\pi f$ and

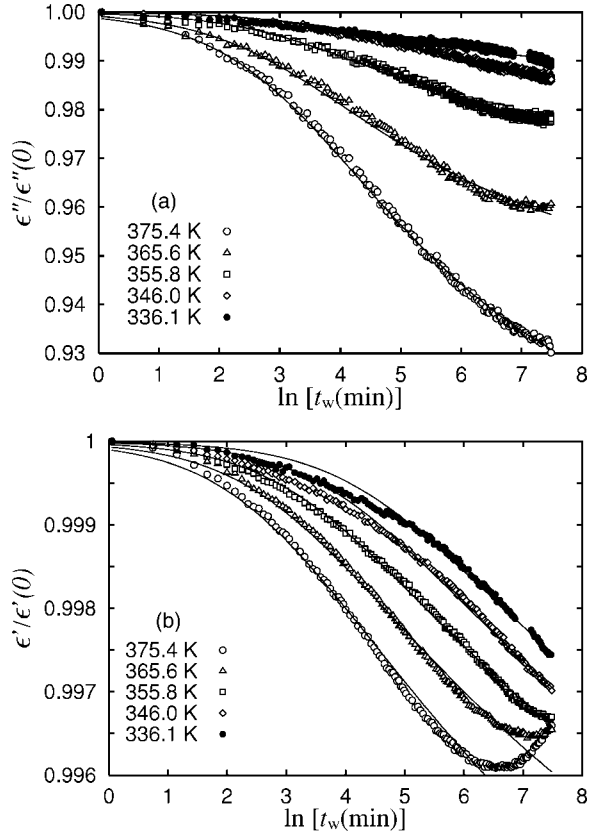

FIG. 1. Aging time dependence of the dynamic dielectric constant normalized with the value at $t_w=0$ in PMMA thin films with $d=20$ nm for various aging temperatures: $T_a=375.4$ K, 365.6 K, 355.8 K, 346.0 K, and 336.1 K: (a) the imaginary component and (b) the real component. The frequency of the applied electric field f is 20 Hz. The horizontal axis is the natural logarithm of t_w. The solid curves are obtained by fitting the data points with Eq. (5). The best-fit parameters for the imaginary parts are listed in Table I.

$$\{t_{w,j}(T_{a,j})\} \equiv \{t_{w,1}(T_{a,1}), t_{w,2}(T_{a,2}), \cdots, t_{w,n}(T_{a,n})\}.$$

If the system is aged for t_w at just one temperature T_a, the dielectric loss at the temperature T is described by

$$\epsilon'' = \epsilon''(T, \omega; t_w(T_a)). \tag{2}$$

First, the aging dynamics under an isothermal condition at $T=T_a$ are considered. In principle, the dielectric loss $\epsilon''(T_a, \omega; \infty)$ is the value of ϵ'' in the equilibrium state at T_a and the rest of ϵ'' can be defined as the aging part $\epsilon''_{ag}(T_a, \omega; t_w)$ in the following way:

$$\epsilon''(T_a, \omega, t_w) = \epsilon''(T_a, \omega; \infty) + \epsilon''_{ag}(T_a, \omega; t_w). \tag{3}$$

The symbols T_a and ω, here, are dropped for simplicity and it is assumed that the aging part of ϵ'' is given by the following equation:

$$\epsilon''_{ag}(t_w) = \frac{\Delta\epsilon''_{ag}}{(1 + t_w/t_0)^n}, \tag{4}$$

where $\Delta\epsilon''_{ag}$ is the relaxation strength towards the equilibrium value, t_0 is the characteristic time of the aging dynamics, and n is an exponent. If t_w is much larger than t_0, $\epsilon''_{ag} \approx t_w^{-n}$. In this case, the dielectric loss ϵ'' decays according to the power-law decay in the long-time region. Similar expressions for ϵ' are also used in this paper.

The solid curves given in Fig. 1(a) were obtained by a nonlinear least-squares fit of the observed data to the following equation derived from Eqs. (3) and (4):

$$\frac{\epsilon''(t_w)}{\epsilon''(0)} = 1 - \frac{\Delta\epsilon''_{ag}}{\epsilon''(0)}\left[1 - \left(1 + \frac{t_w}{t_0}\right)^{-n}\right]. \tag{5}$$

Table I displays the fitting parameters obtained by Eq. (5) for ϵ'' in thin films of PMMA with $d=20$ nm at various aging temperatures, where the value of n is fixed to be the value obtained for 355.8 K. The relaxation strength $\Delta\epsilon''_{ag}$ was found to decrease with decreasing aging temperature T_a. Furthermore, the characteristic time t_0 of the relaxation of ϵ'' in the aging process was found to increase with decreasing T_a; in other words, the aging dynamics become slower with decreasing T_a. Because the observed data in Fig. 1(a) can well be reproduced using Eq. (4), it is implied that the relaxation of ϵ'' at an isothermal condition below T_g obeys the power-law one for the long-time region in the thin films with $d=20$ nm. According to the report in Ref. [10], the aging behavior depends on the frequency of the applied electric field. As the frequency decreases, the relaxation strength due to aging increases for the frequency range from 0.2 Hz to 20 Hz. In this study, we have measured the dynamic dielectric constant over four decades and could confirm the results in Ref. [10].

As mentioned later, under the present experimental conditions that $T_a=336.1-375.4$ K and $f=20$ Hz are located between the α process and β process in the dispersion map. Because $\Delta\epsilon''_{ag}$ decreases with decreasing T_a, the relaxation of

TABLE I. Fitting parameters obtained by fitting the observed values of ϵ'' with Eq. (5) for thin films of PMMA with $d=20$ nm. The frequency of applied electric field is 20 Hz. The exponent n is fixed to be 0.309, which is obtained by fitting the data at 355.8 K

T_a (K)	$\Delta\epsilon''_{ag}/\epsilon''(0)$ ($\times 10^{-2}$)	t_0 (min)	$\epsilon''(0)$	$\Delta\epsilon''_{ag}$
375.4	9.286±0.007	21.8±0.1	0.1147	0.01065
365.6	5.486±0.007	18.6±0.2	0.1302	0.00714
355.8	3.081±0.041	26.4±0.9	0.1601	0.00493
346.0	1.989±0.006	52.3±0.7	0.2016	0.00401
336.1	1.357±0.007	35.3±0.9	0.2495	0.00339

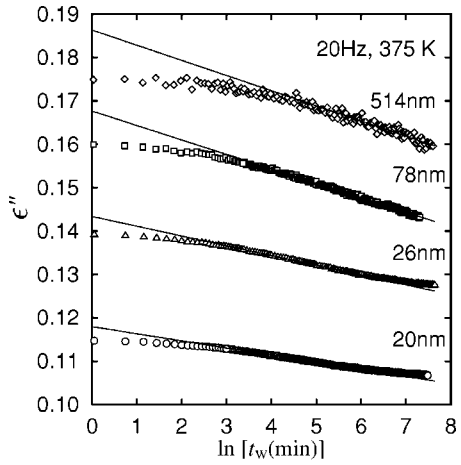

FIG. 2. Aging time dependence of the dielectric loss as a function of film thickness for PMMA thin films: $d=20$ nm, 26 nm, 78 nm, and 514 nm, $T_a=375$ K and $f=20$ Hz. A deviation from the straight line implies that the logarithmic decay does not hold in the long-time region for $d=20$ nm and 26 nm.

ϵ'' due to the aging may be associated with the α process.

Figure 1(b) displays the t_w dependence of the real part of the complex dielectric constant ϵ' normalized with respect to the initial value at various aging temperatures T_a. In this figure, it is found that ϵ' decreases with increasing t_w in a similar way to ϵ'' for T_a's less than 365.6 K. However, there is a surprising difference between ϵ' and ϵ'' for $T_a=375$ K: ϵ' decreases with t_w up to $t_w \approx 11$ h and then begins to increase with t_w. This increase in ϵ' in the long-time region was not observed for lower values of T_a. A similar increase in ϵ' was observed also for $d=26$ nm. On the contrary, for thicker films ($d=78$, 514 nm), no such increase in ϵ' was observed in the present measurements.

We here move to the results for the thin films with various film thickness to see the thickness dependence of the aging dynamics. Figure 2 displays the time variation of the dielectric loss ϵ'' at $T_a=375$ K for the thin films with thickness between 20 nm and 514 nm. Because the horizontal axis in Fig. 2 is on a logarithmic scale, any straight line indicates the existence of a logarithmic decay of the dielectric loss. For $d=20$ nm and 26 nm, we can see that there is a slight deviation from the straight line in the short- and long-time regions. This is consistent with the result that the time variation in ϵ'' obeys Eq. (5) for $d=20$ nm, as shown in Fig. 1(a). For $d=78$ nm and 514 nm, on the other hand, ϵ'' decreases linearly with $\ln t_w$ for the region of $t_w > 20$ min. Within the present time window there is no tendency to saturate to a constant value. In this case, for $t_w > 20$ min, the relaxation of ϵ'' due to aging obeys a logarithmic law. This logarithmic decay law was observed also in the measurements done by Bellon *et al.* [10]. Although it is impossible to judge whether the logarithmic decay is valid also outside the time window, there may be a qualitative difference between the decay law for the thin films and that for the thicker films.

In Sec. III, we have observed that there is the decrease in ϵ' and ϵ'' with increasing t_w at various values of T_a(=336.1–375.4 K), except under the condition that $t_w > 11$ h, $d \leqslant 26$ nm, and $T_a=374$ K, where the increase in ϵ' with t_w was observed. In the discussion section, the physical origin of the time variation of ϵ' and ϵ'' will be discussed.

IV. MEMORY AND REJUVENATION EFFECTS

In Sec. IV we show the memory and rejuvenation effects observed during the aging process and discuss the detailed properties including the thickness dependence. For this purpose, we adopt two modes of thermal history: (i) *Constant-rate mode* (CR mode). After the thermal equilibration at 403 K, the sample is cooled at a rate of 0.5 K/min down to a temperature T_a and then is isothermally annealed (aged) at T_a for 10 h. The sample is then cooled down to room temperature at 0.5 K/min. Finally, the sample is heated again from room temperature to 403 K at 0.5 K/min. (ii) *Temperature-cycling mode* (TC mode). The sample is cooled at a rate of 0.5 K/min from 403 K down to a temperature T_1 and is aged at T_1 for a period of τ_1. Then, the temperature is rapidly changed from T_1 to T_2 ($T_2 \equiv T_1 + \Delta T$) and is kept at T_2 for τ_2. Finally, the temperature is changed back from T_2 to T_1 and is kept at T_1 for τ_3. In this section, we show the data for $\tau_1=\tau_2=5$ h. Both modes were originally developed in order to investigate relaxation behavior in aging phenomena in spin glasses [3–5].

A. Constant-rate mode

As is well known, there are two typical molecular motions in PMMA, which are usually called the α process and β process [23]. The α process is strongly related to the glass transition, while the β process is due to the local motion of polymer chains. In the case of PMMA, the dielectric relaxation strength of the β process is larger than that of the α process due to the existence of polar bulky side groups. Both the dielectric constant and loss have a strong temperature dependence due to the α and β processes. For example, ϵ'' exhibits two distinct loss peaks in a temperature domain at a given frequency: one is at about 310 K due to the β process and the other is at about 400 K due to the α process for $f=20$ Hz and $d=20$ nm (see the inset of Fig. 6.)

For this CR mode, we measured both the dielectric constant ϵ' and the dielectric loss ϵ''. If the range of t_w is restricted to $t_w < 10$ h, there is no qualitative difference in the aging dynamics between ϵ' and ϵ''. In the case of $d=514$ nm, the errors attached to the value of ϵ'' are larger than those of ϵ' because of the resolution of the *LCR* meter. For this reason, we show here the results of ϵ', which can be described as $\epsilon'(T, \omega; t_w(T_a))$ according to our notation. In addition to the ϵ', we prepare a reference curve, $\epsilon'(T, \omega; 0)$, for both the heating and cooling processes at the same rate (0.5 K/min) *without any temporary stop during the cooling process*. We refer to the curve as $\epsilon'_{\rm ref}[\equiv \epsilon'(T, \omega; 0)]$.

Figure 3 shows an example of the temperature dependence of the real part of the complex electric capacitance $\epsilon' C_0$ observed by the CR mode with $T_a=374.2$ K for films with $d=514$ nm. The reference curves $\epsilon'_{\rm ref} C_0$ for the cooling process and the subsequent heating process are given by the solid and dotted curves, respectively. The curve of $\epsilon'_{\rm ref}$ during the cooling process is slightly different from that during the

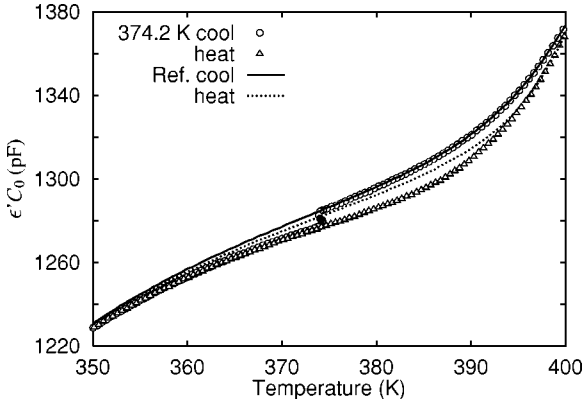

FIG. 3. Temperature dependence of the real part of the complex electric capacitance $\epsilon' C_0$ observed by the CR mode with T_a =374.2 K for PMMA films with d=514 nm. The frequency of the applied electric field f is 20 Hz. The symbols ○ and △ stand for the cooling and heating processes of the CR mode, respectively. The solid curve (−) and dotted curve (···) are for the reference data observed during the cooling and heating processes without any temporary stop at T_a.

heating process. The data points denoted by circles stand for $\epsilon' C_0$ observed during the cooling process, while those denoted by triangles do for $\epsilon' C_0$ observed during the heating process.

Figure 4 displays the temperature change in $\epsilon' - \epsilon'_{\mathrm{ref}}$—i.e., the difference between ϵ' and ϵ'_{ref} obtained by the CR mode with various aging temperatures T_a for d=514 nm. Here, we use ϵ'_{ref} of the cooling (heating) process for ϵ' of the cooling (heating) process. In Fig. 4, it is found that, as the sample is cooled down from 403 K to T_a(=374.2 K), ϵ' is almost equal to ϵ'_{ref} and the difference $\epsilon' - \epsilon'_{\mathrm{ref}}$ remains zero. The difference then begins to deviate from 0 to a negative value and the deviation becomes larger monotonically with increasing aging time (at least up to $t_w \sim 10$ h) during the subsequent isothermal aging at T_a. This indicates that ϵ' decreases with

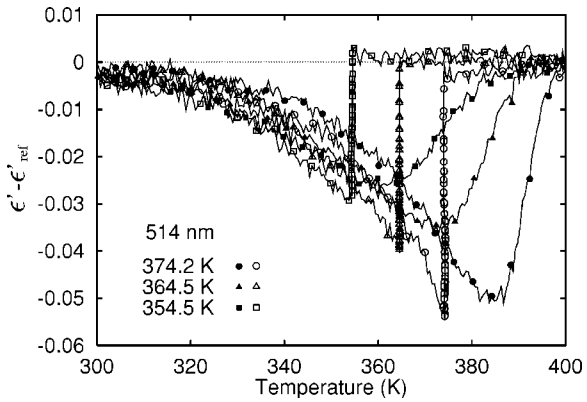

FIG. 4. Temperature dependence of the difference between ϵ' and ϵ'_{ref} observed by CR mode with three different aging temperatures T_a=374.2 K, 364.5 K, and 354.5 K for PMMA films with d =514 nm. The frequency of the applied electric field f is 20 Hz. The heating and cooling rates were 0.5 K/min and the aging times at T_a were 10 h. Open and solid symbols display the data observed during the cooling and heating processes, respectively.

aging time at T_a. As the temperature decreases from T_a to room temperature after the isothermal aging, the difference $\epsilon' - \epsilon'_{\mathrm{ref}}$ decreases with decreasing temperature and becomes almost zero at room temperature. Just after the temperature reaches 293 K, the heating process at the rate of 0.5 K/min starts. As the temperature increases, the difference $\epsilon' - \epsilon'_{\mathrm{ref}}$ begins to deviate from 0 to a negative value almost along the same way as observed during the preceding cooling process. The difference between ϵ' and ϵ'_{ref} exhibits a maximum at around T_a+10 K and then decreases to 0 with increasing temperature.

This behavior observed by the CR mode can be interpreted as follows: the thermal history that the sample is aged at T_a for 10 h is memorized at T_a during the cooling process. As the temperature decreases from T_a to room temperature, the sample begins to rejuvenate and is back to almost a standard age at room temperature. During the subsequent heating process, the sample becomes older almost according to the curve along which the sample experienced rejuvenation during the preceding cooling process after a temporary stop at T_a. This result implies that not only the aging process at T_a near T_g but also the subsequent cooling process can be memorized and the whole thermal history can be read out during the heating process. A similar temperature change in $\epsilon' - \epsilon'_{\mathrm{ref}}$ has already been observed in PMMA films of thickness of 0.3 mm [10].

To investigate the thickness dependence of this aging behavior, we show the results for various film thicknesses, d =26, 78, and 514 nm. In Fig. 5, it is found that the strength of aging for 10 h at 374 K decreases with decreasing film thickness. Furthermore, during the subsequent cooling process, the difference between ϵ' and ϵ'_{ref} approaches zero more quickly in the thin films than in the thicker films. In other words, the thin films are found to age more slowly, but to rejuvenate more quickly.

B. Temperature cycling with negative ΔT

In this subsection, we show the results obtained by the TC mode. In this mode, the sample is aged at two different temperatures T_1 and T_2, and hence ϵ'' is described as the quantity $\epsilon''(T, \omega; t_{w1}, t_{w2})$, where t_{w1} and t_{w2} are the aging times at temperatures T_1 and T_2, respectively. Here, the total aging time t_w is given by $t_w = t_{w1} + t_{w2}$. Using this expression, the dielectric loss ϵ'' observed by the TC mode can be described in the following way:

$$\epsilon'' = \begin{cases} \epsilon''(T_1, \omega; t_w, 0), & 0 < t_w < \tau_1, \\ \epsilon''(T_2, \omega; \tau_1, t_w - \tau_1), & \tau_1 < t_w < \tau_1 + \tau_2, \\ \epsilon''(T_1, \omega; t_w - \tau_2, \tau_2), & t_w > \tau_1 + \tau_2. \end{cases} \tag{6}$$

For example, for a value of $t_w(\tau_1 < t_w < \tau_1 + \tau_2)$, the notation $\epsilon''(T_2, \omega; \tau_1, t_w - \tau_1)$ corresponds to the imaginary part of the dielectric constant observed by frequency $f = \omega/2\pi$ at T_2 after the aging at T_1 for τ_1 and at T_2 for $t_w - \tau_1$. In this case, the reference curve $\epsilon''_{\mathrm{ref}}$ can also be defined as $\epsilon''_{\mathrm{ref}} = \epsilon''(T, \omega; 0, 0)$.

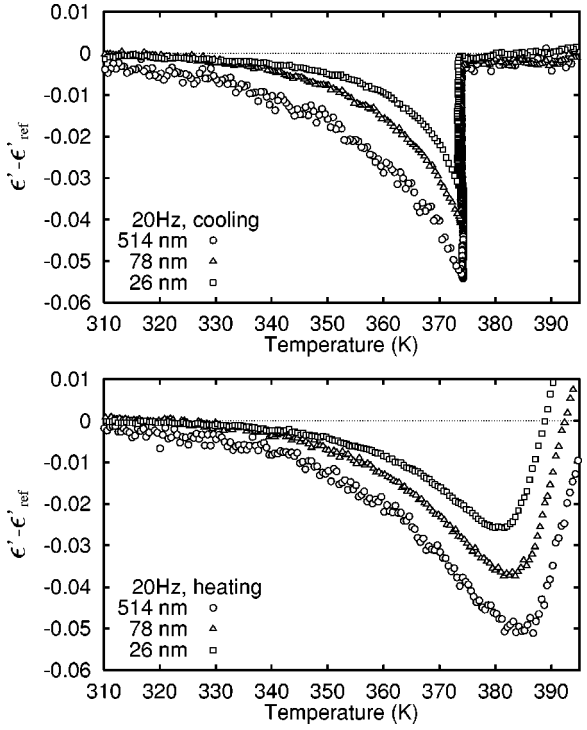

FIG. 5. Difference between ϵ' and ϵ'_{ref} as functions of temperature observed by the CR mode for PMMA thin films with $d=26$ nm, 78 nm, and 514 nm. The upper figure displays the results for the cooling process and the lower one those for the subsequent heating process. Dielectric measurements were done for $f=20$ Hz. The isothermal aging was done at $T_a=374$ K during the cooling process.

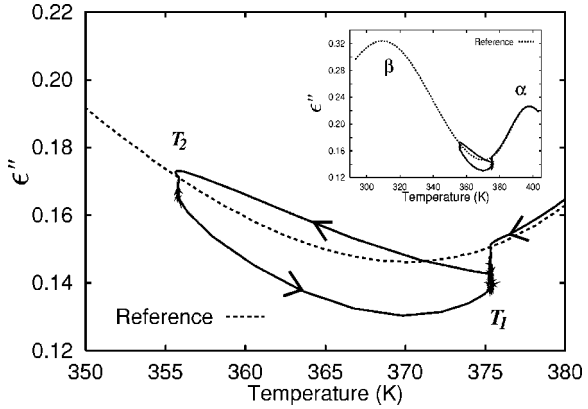

FIG. 6. Temperature dependence of the dielectric loss observed by the TC mode with $T_1=375.3$ K and $T_2=355.8$ K ($\Delta T=-19.5$ K) for PMMA thin films with $d=20$ nm and the frequency of the applied electric field $f=20$ Hz. The dotted curve displays the temperature dependence of ϵ'' obtained during the cooling process with the rate of 0.5 K/min without any isothermal aging. The overall behavior of ϵ'' for temperature range from 310 K to 403 K is shown in the inset.

Figure 6 displays a typical behavior of ϵ'' and $\epsilon''_{\mathrm{ref}}$ of the TC mode for PMMA thin films with $d=20$ nm and $f=20$ Hz. In the inset, the temperature dependence of $\epsilon''_{\mathrm{ref}}$ at 20 Hz is shown for the temperature range from 290 K to 403 K during the cooling process (see the dotted curve). The two distinct loss peaks, the α process and β process, are observed. As the sample is cooled from 403 K to T_1(=375.3 K) at the rate of 0.5 K/min according to the procedure of the TC mode, the dielectric loss ϵ'' moves along the reference curve $\epsilon''_{\mathrm{ref}}$ and then deviates from the reference curve to a lower value upon the beginning of the aging at T_1 (see the solid curve). The main part of Fig. 6 shows this behavior in the temperature range from 350 K to 380 K. As the temperature decreases from T_1 to T_2 (=355.8 K) by $\Delta T=-19.5$ K after the aging at T_1 for a period of τ_1, the dielectric loss ϵ'' immediately returns to a value on the reference curve at T_2. As the temperature is kept at T_2, ϵ'' deviates from the value on the reference curve. While the temperature is changed from T_2 to T_1 and is kept at T_1 after the aging at T_2 for a period of τ_2, ϵ'' goes back to a value at T_1, which deviates from the reference curve, and then ϵ'' decreases with time during the aging process at T_1.

To elucidate the aging dynamics at a temperature in the TC mode more in detail, it is useful to investigate the difference between ϵ'' and $\epsilon''_{\mathrm{ref}}$ as we have already done in the CR mode. In this case, the reference values $\epsilon''_{\mathrm{ref}}(T_j,\omega)$ at T_j ($j=1,2$) are subtracted from the observed dielectric losses ϵ'' at T_j, respectively. Here, we define $\epsilon''-\epsilon''_{\mathrm{ref}}\equiv\epsilon''(T,\omega;t_{w1},t_{w2})-\epsilon''_{\mathrm{ref}}(T,\omega;0,0)$, where $t_w=t_{w1}+t_{w2}$. For the TC mode,

$$\epsilon''-\epsilon''_{\mathrm{ref}}\equiv\epsilon''(T,\omega;t_{w1},t_{w2})-\epsilon''_{\mathrm{ref}}(T,\omega;0,0)=\begin{cases}\epsilon''(T_1,\omega;t_w,0)-\epsilon''_{\mathrm{ref}}(T_1,\omega;0,0), & 0<t_w<\tau_1,\\ \epsilon''(T_2,\omega;\tau_1,t_w-\tau_1)-\epsilon''_{\mathrm{ref}}(T_2,\omega;0,0), & \tau_1<t_w<\tau_1+\tau_2,\\ \epsilon''(T_1,\omega;t_w-\tau_2,\tau_2)-\epsilon''_{\mathrm{ref}}(T_1,\omega;0,0), & t_w>\tau_1+\tau_2.\end{cases} \tag{7}$$

Figure 7 displays the time dependence of $\epsilon''-\epsilon''_{\mathrm{ref}}$ for the thin films with $d=20$ nm, $T_1=375.3$ K, $T_2=355.8$ K, and $\Delta T=-19.5$ K. The origin of the time ($t_w=0$) is defined as the time when the temperature reaches T_1 after the cooling from 403 K (above T_g). The value of $\epsilon''-\epsilon''_{\mathrm{ref}}$ is found to decrease with increasing t_w and to change immediately to 0 when the temperature is lowered from T_1 to T_2 at $t_w=\tau_1$. This indicates that the decrease in temperature from T_1 to T_2 causes the polymer sample to *rejuvenate*. As the aging time elapses at T_2 after the temperature shift, $\epsilon''-\epsilon''_{\mathrm{ref}}$ is found to exhibit a relaxation just like a new relaxation process starts at $t_w=\tau_1$. The dotted curve in Fig. 7(a) which starts at $t_w=\tau_1$ is the

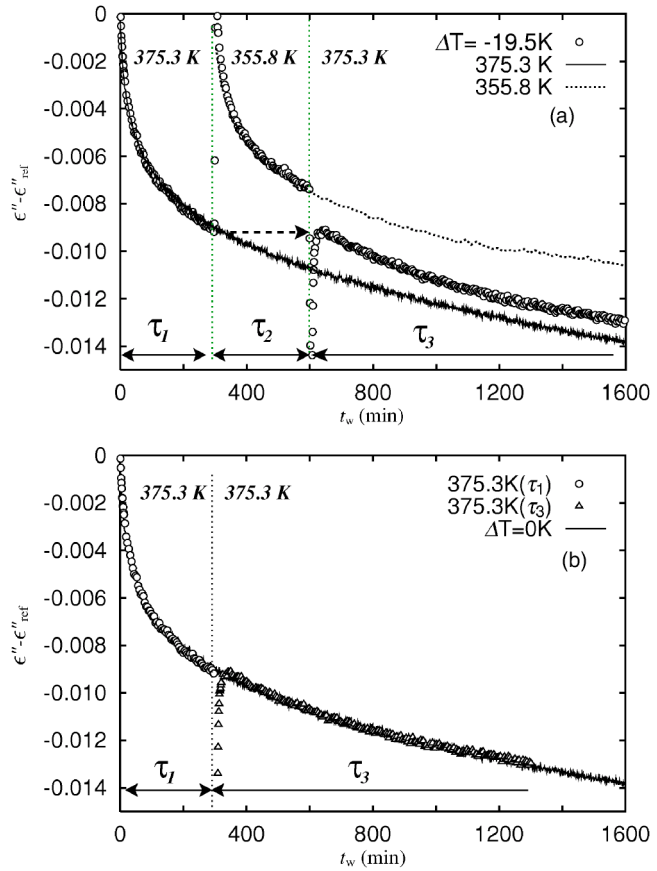

FIG. 7. (a) Difference between ϵ'' and $\epsilon''_{\mathrm{ref}}$ observed by the TC mode with $T_1=375.3$ K and $T_2=355.8$ K ($\Delta T=-19.5$ K) for PMMA thin films with $d=20$ nm. (b) The difference $\epsilon''-\epsilon''_{\mathrm{ref}}$ obtained by shifting the data points in the third stage in the negative direction of the time axis by τ_2 after removing the data points in the second stage. Aging times at the first and second stages are $\tau_1=\tau_2=5$ h. The horizontal axis of (b) is the total aging time at T_1. The solid (—) and dotted curves (···) are standard relaxation ones obtained by isothermal aging at $T_1=375.3$ K and $T_2=355.8$ K, respectively. It should be noted that the time origin of the dotted curve for T_2 is shifted from $t_w=0$ to $t_w=\tau_1$.

relaxation curve of $\epsilon''-\epsilon''_{\mathrm{ref}}$ observed at T_2 after the temperature change directly from 403 K to T_2. The origin of the time axis is shifted from 0 to $t_w=\tau_1$ for the dotted curve in Fig. 7(a). The observed data for $\tau_1<t_w<\tau_1+\tau_2$ are located exactly upon this dotted curve. At $t_w=\tau_1+\tau_2$, the system is heated up to T_1, and then the temperature of the system is kept at T_1. On this stage, $\epsilon''-\epsilon''_{\mathrm{ref}}$ is found to go back to the value which $\epsilon''-\epsilon''_{\mathrm{ref}}$ had reached at $t_w=\tau_1$ and to begin to decrease as if there were no temperature change during the aging process at T_1.

In Fig. 7(b) is shown the time evolution of $\epsilon''-\epsilon''_{\mathrm{ref}}$ after removing the data between τ_1 and $\tau_1+\tau_2$ and shifting the data for $t_w>\tau_1+\tau_2$ in the negative direction along the time axis by τ_2. We can consider the horizontal axis as the total time which the system spent at T_1. In this figure, we can see that $\epsilon''-\epsilon''_{\mathrm{ref}}$ decreases monotonically with the aging time without any discontinuous change except for a short region just after $t_w=\tau_1$. The curve obtained in the above way agrees very well with that obtained by keeping the system at T_1 without any temperature change, $\epsilon''(T_1,\omega;t_w,0)-\epsilon''_{\mathrm{ref}}(T_1,\omega;0,0)$ (we call this curve *the standard relaxation curve*). This implies that polymer glasses can remember the state at $t_w=\tau_1$ of the relaxation towards the equilibrium state and recall the memory at $t_w=\tau_1+\tau_2$. We call this behavior a *complete memory effect*. This was a result obtained for $\Delta T=-19.5$ K.

We show here the aging behavior for various values of ΔT for PMMA thin films with $d=26$ nm. Figures 8(a)–8(d) show $\epsilon''-\epsilon''_{\mathrm{ref}}$ as a function of the aging time t_w for various values of from $\Delta T=-19.6$ K to -4.8 K and $T_1=374.2$ K. Figures 8(e)–8(h) are obtained from Figs. 8(a)–8(d) according to the following procedure: the data points for $t_w=\tau_1\sim\tau_1+\tau_2$ are removed and the ones for $t_w>\tau_1+\tau_2$ are shifted by an amount of $\Delta\tau$ in the negative direction along the t_w axis so that the data can be overlapped with the standard relaxation curve for aging at T_1 in the most reasonable way. Here, an effective time τ_{eff} is defined as the time $\tau_2-\Delta\tau$. The effective time can be considered as a measure of the contributions of the aging at T_2 to that at T_1. If τ_{eff} is zero, the aging at T_2 has no contributions to that at T_1, while if τ_{eff} is equal to τ_2, the aging at T_2 has full contributions to that at T_1. In Figs. 8(a)–8(d), it is found that the value of $\epsilon''-\epsilon''_{\mathrm{ref}}$ is reinitialized at $t_w=\tau_1$ for from $\Delta T=-19.6$ K to -9.9 K. However, the reinitialization at $t_w=\tau_1$ is not complete for $\Delta T=-4.8$ K.

As shown in Figs. 8(e)–8(h), $\tau_{\mathrm{eff}}=0$ for from $\Delta T=-19.6$ K to -9.9 K and $\tau_{\mathrm{eff}}\approx 200$ min for $\Delta T=-4.8$ K. This indicates that for $|\Delta T|\geqslant 9.9$ K there is a complete memory effect and the aging at T_2 gives no contributions to that at T_1; in other words, the aging at T_1 is independent of that at T_2. On the contrary, for $\Delta T=-4.8$ K, the aging at T_2 is no longer independent of that at T_1, but gives some contributions to that at T_1. As a result, τ_{eff} has a positive finite value. It should be noted here that, although the above result is obtained for ϵ'', almost similar results are obtained also for ϵ'.

Next, we show the result obtained for PMMA films with $d=514$ nm, which is much larger than $d=26$ nm. As an example, the observed results of ϵ' for $f=100$ Hz are shown in Fig. 9. It is found from Figs. 9(e)–9(h) that for $\Delta T=-19.7$ K, τ_{eff} is zero; that is, the aging dynamics at T_1 is totally independent of that at T_2. However, as $|\Delta T|$ decreases, τ_{eff} increases monotonically. For $\Delta T=-4.7$ K, $\tau_{\mathrm{eff}}\approx\tau_2$. This means that the aging at T_2 has almost full contributions to that at T_1. On the basis of these results, it can be expected that the contributions of the aging at T_2 to that at T_1 change continuously with decreasing $|\Delta T|$. A similar continuous change in τ_{eff} with respect to $|\Delta T|$ has also been observed in some examples of spin glasses [24,25]. Comparing Fig. 8 with Fig. 9, it is found that thinner PMMA films are more sensitive to the change in $|\Delta T|$ than thicker PMMA films.

To measure the contributions of the aging at T_2 to that at T_1, we evaluate the ratio $\tau_{\mathrm{eff}}/\tau_2$ as functions of ΔT under various conditions. In the case of $d=514$ nm, we use the values of ϵ' for $f=100$ Hz and 20 Hz and those of ϵ'' for $f=100$ Hz, while in the case of $d=26$ nm, we use the values of ϵ' for $f=20$ Hz and those of ϵ'' for $f=20$ Hz. Figure 10 displays that the effective time τ_{eff} normalized with τ_2 is a decreasing function of $|\Delta T|$ and decays to zero as $|\Delta T|$

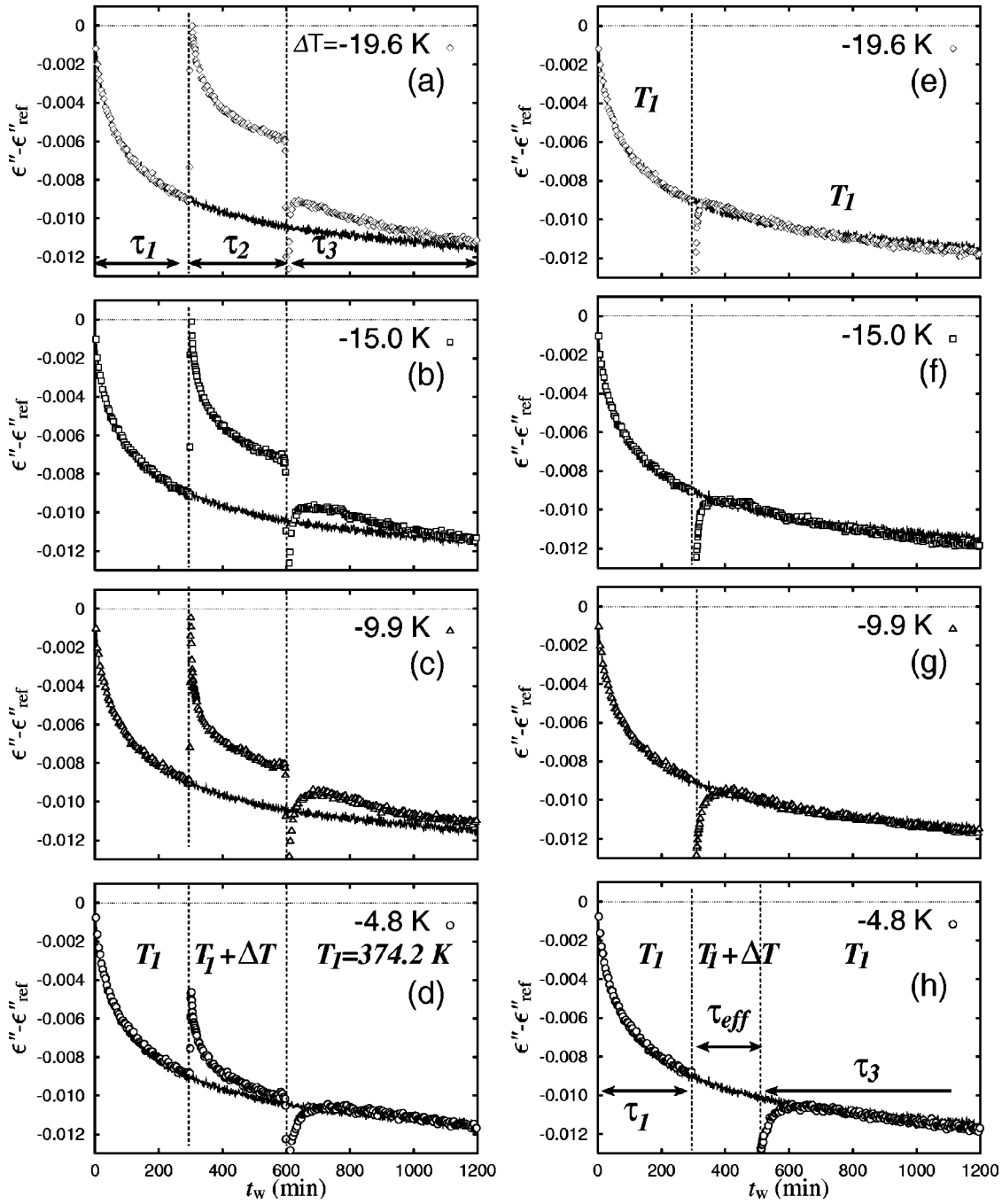

FIG. 8. Difference between ϵ'' and $\epsilon''_{\mathrm{ref}}$ observed by the TC mode for PMMA thin films with $d=26$ nm and $f=20$ Hz. The aging temperature of the first stage T_1 is fixed to be 374.2 K and T_2 ($\equiv T_1+\Delta T$) is changed: $\Delta T=-4.8$ K (d),(h), -9.9 K (c),(g), -15.0 K (b,),(f), and -19.6 K (a),(e). Aging times are $\tau_1=\tau_2=5$ h. In (e)–(h), the data points of the second stages are removed and those of the third stage are shifted by an amount of time in the negative direction of the time axis so that the data points of the third stages can be overlapped with the standard relaxation curve most reasonably. The effective time τ_{eff} is evaluated as the difference between the time at the end of the first stage and the time at the beginning of the initial time of the third stage after the above data fitting process. The difference in length between the arrow of τ_2 in (a) and the arrow of τ_{eff} in (h) shows how the aging at T_2 affects the aging at T_1.

increases. The decaying rate of $\tau_{\mathrm{eff}}/\tau_2$ with respect to $|\Delta T|$ is larger for $d=26$ nm than for $d=514$ nm. Therefore, we can say that the independence of the aging dynamics between two different temperatures is accomplished faster in thinner films with increasing $|\Delta T|$.

It is interesting to compare the ΔT dependence of τ_{eff} with that estimated through a thermal activation process [26]. If it is assumed that the aging involves a thermally activated jump over a free energy barrier ΔU, the corresponding time τ at temperature T characteristic of the jump motion over the barrier is given by $\tau(T)=\tau_0 \exp(\Delta U/k_B T)$, where τ_0 is a microscopic time scale and k_B is the Boltzmann constant. Here, we consider the aging at T_2 for a period of τ_2. In this case, we can say that the aging process proceeds by a reduced time

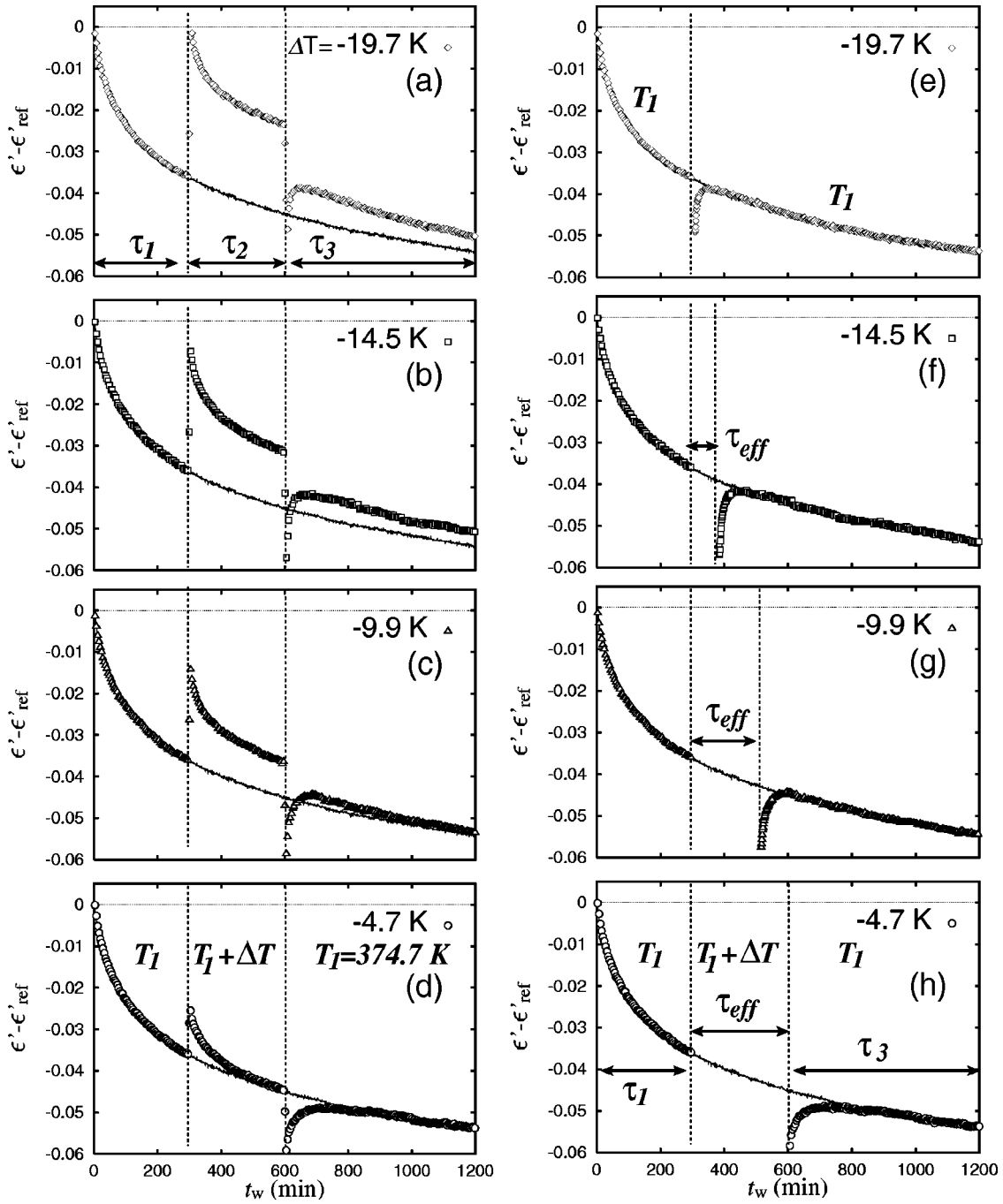

FIG. 9. Difference between ϵ' and ϵ'_{ref} observed by the TC mode for PMMA films with $d=514$ nm and $f=100$ Hz. The aging temperature of the first stage T_1 is fixed to be 374.7 K and T_2 ($\equiv T_1+\Delta T$) is changed: $\Delta T=-4.7$ K (d),(h), −9.9 K (c),(g), −14.5 K (b),(f), and −19.7 K (a),(e). Aging times are $\tau_1=\tau_2=5$ h. In the right figures, τ_{eff} is the same as defined in Fig. 8.

$\tilde{\tau}$ [$\equiv \tau_2/\tau(T_2)$]. If the reduced time $\tilde{\tau}$ of a state is the same as that of another state, we can consider that both the states are the same. Because the aging process at T_2 for a period of τ_2 corresponds to that at T_1 for a period of τ_{eff}, we obtain the relation $\tau_{\mathrm{eff}}/\tau(T_1)=\tau_2/\tau(T_2)$. If the energy barrier ΔU is independent of T, we obtain the relation $[\tau(T_1)/\tau_0]^{T_1}=[\tau(T_2)/\tau_0]^{T_2}$ for the thermal activation process. Combining the above two equations, we obtain the relation for the temperature shift from T_2 ($=T_1+\Delta T$) to T_1:

$$\frac{\tau_{\mathrm{eff}}}{\tau_2}=\left(\frac{\tau(T_2)}{\tau_0}\right)^{\Delta T/T_1}. \tag{8}$$

Because the determination of τ_{eff} is accompanied with the relatively large uncertainty, it is difficult to judge whether Eq. (8) can reproduce the observed data in Fig. 10. Nevertheless, from the qualitative comparison of the observed results with Eq. (8), it is found that the microscopic time τ_0

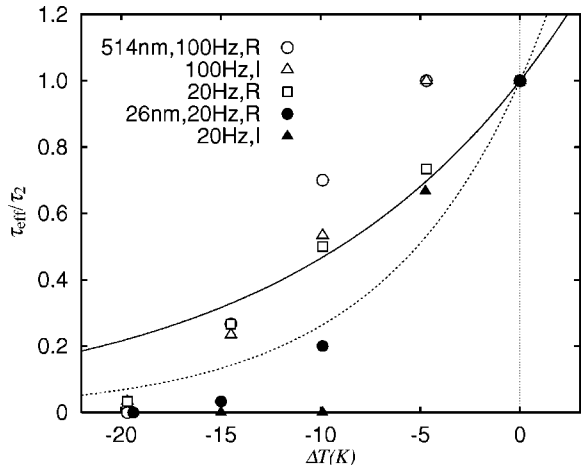

FIG. 10. Dependence of effective time $\tau_{\rm eff}$ normalized with the aging time of the second stage τ_2 on the difference of two aging temperatures for PMMA thin films with $d=26$ nm, 514 nm and $f=20$ Hz, 100 Hz. The effective time $\tau_{\rm eff}$ is evaluated from the data for ϵ' and ϵ''. Open and solid symbols display the results for $d=514$ nm and $d=26$ nm, respectively. The curves are obtained by fitting the data to Eq. (8). The solid curve is for $d=514$ nm and the dotted curve is for $d=26$ nm.

associated with the aging is smaller in thin-film geometry than in the bulk films.

V. DISCUSSIONS

A. Physical origin of the t_w dependence of ϵ' and ϵ''

As shown in Sec. III, we have observed the interesting behavior of the aging dynamics. In this section we discuss the physical origin of the t_w dependence of ϵ' and ϵ'' observed in the present measurements. The dynamic dielectric constant $\epsilon^*(T)$ is obtained by dividing the complex electric capacitance $C^*(T)$ at the temperature T by the geometrical capacitance $C_0(T_0)$ evaluated at $T_0=273$ K.

The evaluation of ϵ^* in this paper is based on the assumption that the T and t_w dependence of C_0 can be neglected compared with that of the *intrinsic* dielectric constant. This assumption may not be valid in some cases. The T dependence of C_0 can be neglected as long as the value normalized with that at $t_w=0$ is used for a given temperature. However, the t_w dependence of C_0 cannot be neglected for the following two reasons. First, it is well known that the physical aging of polymers increases the density with aging time. This is called densification, which leads to a decrease in film thickness with increasing t_w. This contraction should be commonly observed independent of film thickness. In addition to this, recent measurements done by Miyazaki and co-workers show that the film thickness of polystyrene (PS) thin films supported on Si substrate decreases very slowly with time at an annealing temperature above T_g when the initial thickness is less than 20 nm [27,28]. This indicates that there should be a very slow relaxation process of PS in *thin-film geometry*. If we take into account the above two processes for PMMA thin films, it follows that the geometrical capacitance C_0 depends on the aging time t_w and that the t_w dependence of C_0 of ultrathin films can be different from that of bulk samples.

The effect due to the t_w dependence of C_0 is evaluated here. Since $C'=\epsilon'\epsilon_0 S/d$, the relative change in C' is given by

$$\frac{\Delta C'}{C'}=\frac{\Delta\epsilon'}{\epsilon'}-\frac{\Delta d}{d}, \tag{9}$$

where S is assumed not to change with time and the symbol ΔX $(X=C',\epsilon',d)$ is $\Delta X\equiv X(t_w)-X(0)$. The discussions in this paragraph can also be valid for ϵ'' and C''. If the sample goes towards an equilibrium state during the aging process at a temperature, the densification proceeds and the thermal fluctuations are suppressed. The former leads to a decrease in d, while the latter leads to a decrease in ϵ'. In this case, it is reasonable to expect that $\Delta d/d$ and $\Delta\epsilon'/\epsilon'$ have the same form with respect to t_w. Although the aging strength may be modified, we can evaluate the t_w dependence of ϵ' through that of C'. In thin-film geometry, however, the t_w dependence of ϵ' obtained thus may be affected by the possible existence of a very slow relaxation process of a film thickness.

As shown in Fig. 1(b), we observed that $\epsilon'[\equiv C'(T)/C'_0(T_0)]$ *increases* with t_w after decaying up to about 11 h during the aging at $T_a=375.4$ K for PMMA thin films with initial thickness of 20 nm. This increase may be due to the existence of a very slow relaxation process of the thickness observed only in thin-film geometry [27]. The characteristic time of this very slow relaxation process should be longer than that of the relaxation of the *intrinsic* $\epsilon'(\epsilon'')$ and the contraction due to the physical aging.

Now let us try to estimate the effect of the existence of this very slow relaxation process on the present experimental results. Comparing the results in Figs. 1(a) and 1(b), we find that $\Delta\epsilon''(t_w)/\epsilon''(0)\sim 0.062$ and $\Delta\epsilon'(t_w)/\epsilon'(0)\sim 0.0048$ for $t_w=11$ h at $T_a=375.4$ K. An analysis of $\Delta d/d$ in the present measurements shows that $\Delta d(t_w)/d(0)\sim 0.0009$ for $t_w=11$ h at $T_a=375.4$ K. Therefore, even if the increase in ϵ' exists under some conditions, the effect of this increase on the dynamics of the intrinsic ϵ' is less than 20% when t_w is limited to $t_w<11$ h. It should be noted here that this effect can only be observed for ϵ' near T_g and for ultrathin films $(d=20,26$ nm). On the basis of this discussion, we believe that the observed dynamics of ϵ' and ϵ'' in the present measurements can safely be regarded as those of the intrinsic dielectric constants for PMMA thin films, except for some special conditions mentioned above.

The discussions here are based on the existence of the very slow relaxation mode in PMMA thin films. In order to check the validity of this assumption, we should measure the frequency spectrum of dynamics dielectric constant in the lower-frequency region.

B. Comparison with the aging scenario in spin glasses

In the CR and TC modes, we observed memory and rejuvenation effects. There are many common properties between polymer glasses and spin glasses. For spin glass systems, the memory and rejuvenation effects have been discussed by two different models: one is a hierarchical model [3,4] and the other is a droplet model [29–32].

The hierarchical model is based on the mean-field picture originating from the Sherrington-Kirkpatrick model [33]. It is assumed that the spin glass (SG) phase is characterized by a multivalley structure of the free-energy surface at a given temperature. At a temperature T_1, the system relaxes over the many valleys formed at that temperature. When the system is cooled from T_1 to $T_1+\Delta T$ ($\Delta T<0$), each valley of the free energy splits into new smaller subvalleys. If $|\Delta T|$ is large enough, the energy barriers separating the initial valleys are too high to go among different initial valleys within the period of τ_2 at $T_1+\Delta T$. Only relaxations within the initial valleys can be activated, and hence the occupation number of each initial valley holds during the aging at $T_1+\Delta T$. When the system is heated again from $T_1+\Delta T$ to T_1, the small subvalleys merge back into their ancestors. Therefore, the memory at the end of the first isothermal aging process at T_1 can be memorized and recalled at $\tau_1+\tau_2$. The rejuvenation effects can also be explained in a similar way.

As for the droplet model, the growth of the SG-ordered domain is taken into account. In a spin glass system, the growth rate of the domain is very slowed down because of the heterogeneous distribution of the frustration. Furthermore, the memory and rejuvenation effects can be explained within the droplet theory using the *temperature chaos concept*, in which the spin configuration or the energy landscape can be changed globally even for any infinitesimal temperature change on a length scale larger than the *overlap length*.

Recent studies based on the droplet model produced more powerful scenarios such as the droplets-in-domain scenario [34] and the ghost domain scenario [35,36]. Furthermore, disordered systems showing the memory effects have been classified into two categories as follows.

(i) The system showing strong rejuvenation effects and memory effects: the *strong rejuvenation* is due to the temperature chaos effect. The relaxation associated with the strong rejuvenation after the temperature shift from T_1 to T_2 is the same as that observed after the direct cooling to the aging temperature T_2.

(ii) The system showing no strong rejuvenation, but a transient relaxation and memory effects: in this case, the strength of the transient relaxation after the temperature shift by ΔT becomes stronger with increasing $|\Delta T|$. The aging proceeds cumulatively even if the temperature is shifted.

In some systems, both properties can be observed depending on the temperature shift ΔT. For a sufficiently small ΔT the aging proceeds cumulatively. When ΔT becomes large, the aging is no longer cumulative but the noncumulative and strong rejuvenation is observed just after the temperature shift.

Polymeric systems have been so far classified into the type (ii). Although the memory effects have been observed, it has been reported in the literature that no strong rejuvenation occurs after the temperature shift [35]. However, the present measurements show that, after the negative temperature shift from T_1 to T_2 by $\Delta T\approx -20$ K, the relaxation of ϵ'' due to the aging is reinitialized—i.e., goes back to the value on the reference curve measured during the cooling process. The values of the ϵ'', then, begin to decay at T_2 along the relaxation curve measured after the cooling directly to T_2, as shown in Fig. 7. From these results, we believe that there is a strong rejuvenation in the case of PMMA for $\Delta T\approx -20$ K. Furthermore, as ΔT decreases from -4.8 K to -19.6 K in Fig. 8, the contributions of the aging at T_2 to that at T_1 decrease, and the effective time τ_{eff} decreases to 0 with increasing $|\Delta T|$ in the negative-temperature cycle. These experimental results imply that there is a crossover from the cumulative dynamics to the noncumulative one as the value of $|\Delta T|$ increases. In order to check whether there is really a crossover from cumulative to noncumulative—i.e., whether there is the temperature chaos effect in polymeric systems—"twin-temperature shift" experiments should be performed, which have been developed in spin glasses [37].

Comparing polymeric systems with spin glasses, the characteristic time of the microscopic flip motion of dipoles or spins can be expected to be much larger in polymeric systems than in spin glasses. Therefore, polymeric systems may be a model system for investigating the aging dynamics in the shorter-time regime, since an experimental time window corresponds to shorter time scales in polymeric systems compared with atomic spin glasses. Superspin glasses (strongly interacting nanoparticle systems) [25] can also be regarded as a model system for the same purpose, because they have the longer microscopic flip time of a superspin than atomic spin glasses have. The polymeric systems may have a still longer microscopic flip time, and hence we expect that the polymeric systems can be better model systems.

C. Thickness dependence of aging dynamics

As for the thickness dependence of the aging phenomena, we could obtain several interesting results: (i) The relaxation strength due to the aging decreases with decreasing film thickness. (ii) The width of the dip in $\epsilon'-\epsilon'_{\mathrm{ref}}$ during the cooling process in the CR mode becomes smaller with decreasing film thickness. (iii) The effective time τ_{eff} in the TC mode decays to zero more quickly in a thin-film geometry with increasing $|\Delta T|$ in the negative-ΔT region than in bulk systems.

As mentioned in Sec. IV, some of the above results relating to the thickness dependence may be explained by assuming that the fundamental microscopic flip time τ_0 of dipoles becomes smaller with decreasing film thickness. As shown in Fig. 5, the width of the dip observed during the cooling process in the CR mode is $\sim$20 K for $d=514$ nm and $\sim$10 K for $d=26$ nm in the case of PMMA films. In (atomic) spin glasses, where τ_0 is much smaller than in polymer glasses, the width of the dip of ϵ' in the CR mode is $\sim$3 K [25], which is even smaller than the value for the thinnest-film thickness. The width of the dip observed in the CR mode does not depend on the cooling rate for the range of cooling rate from 0.08 K/min to 0.33 K/min, although the depth of the dip strongly depends on the cooling rate [10].

VI. SUMMARY

In this paper, we have investigated the aging dynamics in thin films of PMMA with $d=20-514$ nm through dielectric measurements. The results obtained in the present measurements are as follows.

(i) The relaxation of dielectric constants is observed during the aging process at an aging temperature T_a. The relaxation strength decreases with decreasing T_a and with decreasing film thickness. In the films of $d=20$ nm and 26 nm, an increase in ϵ' has been observed at $T_a=375$ K, which may be due to the existence of the ultraslow relaxation process of the film thickness observed recently through the x-ray reflectivity measurements.

(ii) In the CR mode, the aging at T_a by the way of cooling to room temperature can be memorized as the dip in $\epsilon' - \epsilon'_{\mathrm{ref}}$ curve around T_a. During the subsequent heating process the memory can be recalled. The width of the dip in $\epsilon' - \epsilon'_{\mathrm{ref}}$ decreases with decreasing film thickness.

(iii) In the TC mode with negative ΔT, a strong rejuvenation effect of the difference between ϵ'' and $\epsilon''_{\mathrm{ref}}$ has been observed just after the negative shift from T_1 to T_2 by $\Delta T \approx -20$ K. At the same time, a complete memory effect could also be observed when the temperature goes back from T_2 to T_1.

(iv) As $|\Delta T|$ decreases in the negative-ΔT region in the TC mode, the contributions of the aging at T_2 to that at T_1 become larger; i.e., the effective time τ_{eff}, which is a measure of the contribution, increases from 0 to τ_2. A continuous change in τ_{eff} with ΔT could be observed, which reminds us of a crossover between the noncumulative aging and the cumulative one. The dependence of τ_{eff} on ΔT depends on the film thickness.

In this paper, we focused on the aging dynamics observed in dielectric constants. However, similar aging phenomena can also be observed in heat capacity of PMMA observed by temperature modulated DSC [38]. It can be expected that the aging phenomena observed in this paper are common ones for any susceptibility including dielectric constant, magnetic susceptibility, and heat capacity.

ACKNOWLEDGMENTS

The authors appreciate H. Yoshino and H. Takayama for useful discussions. This work was supported by a Grant-in-Aid for Scientific Research (B) (No. 16340122) from the Japan Society for the Promotion of Science and for Exploratory Research (No. 16654068) from the Ministry of Education, Culture, Sports, Science and Technology of Japan.

[1] L. C. Struick, *Physical Aging in Amorphous Polymers and Other Materials* (Elsevier, New York, 1978).
[2] J.-P. Bouchaud, in *Soft and Fragile Matter*, edited by M. E. Cates and M. R. Evans (IOP Publishing, Bristol, 2000), p. 185.
[3] F. Lefloch, J. Hammann, M. Ocio, and E. Vincent, Europhys. Lett. **18**, 647 (1992).
[4] E. Vincent, J.-P. Bouchaud, J. Hamman, and F. Lefloch, Philos. Mag. B **71**, 489 (1995).
[5] K. Jonason, E. Vincent, J. Hammann, J. P. Bouchaud, and P. Nordblad, Phys. Rev. Lett. **81**, 3243 (1998).
[6] K. Jonason, P. Nordblad, E. Vincent, J. Hammann, and J.-P. Bouchaud, Eur. Phys. J. B **13**, 99 (2000).
[7] P. Doussineau, T. de Lacerda-Aroso, and A. Levelut, Europhys. Lett. **46**, 401 (1999).
[8] R. L. Leheny and S. R. Nagel, Phys. Rev. B **57**, 5154 (1998).
[9] O. Kircher and R. Böhmer, Eur. Phys. J. B **26**, 329 (2002).
[10] L. Bellon, S. Ciliberto, and C. Laroche, Eur. Phys. J. B **25**, 223 (2002).
[11] L. Bellon, S. Ciliberto, and C. Laroche, e-print cond-mat/9905160.
[12] *Proceedings of the 4th International Discussion Meeting on Relaxations in Complex Systems* [J. Non-Cryst. Solids 307–310, 1 (2002)].
[13] A. J. Kovacs, J. J. Aklonis, J. M. Hutchinson, and A. A. Ramos, J. Polym. Sci., Polym. Phys. Ed. **17**, 1097 (1979).
[14] Y. Miyamoto, K. Fukao, H. Yamao, and K. Sekimoto, Phys. Rev. Lett. **88**, 225504 (2002).
[15] J. L. Keddie, R. A. L. Jones, and R. A. Cory, Europhys. Lett. **27**, 57 (1994).
[16] K. Fukao and Y. Miyamoto, Phys. Rev. E **61**, 1743 (2000).
[17] K. Fukao and Y. Miyamoto, Phys. Rev. E **64**, 011803 (2001).
[18] K. Fukao, S. Uno, Y. Miyamoto, A. Hoshino, and H. Miyaji, Phys. Rev. E **64**, 051807 (2001).
[19] *Proceedings of the 2nd International Workshop on Dynamics in Confinement* [Eur. Phys. J. E12, 1 (2003)].
[20] S. Kawana and R. A. L. Jones, Eur. Phys. J. E **10**, 223 (2003).
[21] A. Angell, Nature (London) **393**, 521 (1998).
[22] P. G. Debenedetti and F. H. Stillinger, Nature (London) **410**, 259 (2001).
[23] N. G. McCrum, B. E. Read, and G. Williams, *Anelastic and Dielectric Effects in Polymeric Solids* (Wiley, London, 1967).
[24] M. Sasaki, V. Dupuis, J.-P. Bouchaud, and E. Vincent, Eur. Phys. J. B **29**, 469 (2002).
[25] P. E. Jönsson, H. Yoshino, H. Mamiya, and H. Takayama, Phys. Rev. B **71**, 104404 (2005).
[26] V. Dupuis, E. Vincent, J.-P. Bouchaud, J. Hammann, A. Ito, and H. Aruga Katori, Phys. Rev. B **64**, 174204 (2001).
[27] T. Kanaya, T. Miyazaki, H. Watanabe, K. Nishida, H. Yamano, S. Tasaki, and D. B. Bucknall, Polymer **44**, 3769 (2003).
[28] T. Miyazaki, K. Nishida, and T. Kanaya, Phys. Rev. E **69**, 022801 (2004).
[29] A. J. Bray and M. A. Moore, Phys. Rev. Lett. **58**, 57 (1987).
[30] D. S. Fisher and D. A. Huse, Phys. Rev. B **38**, 373 (1988).
[31] D. S. Fisher and D. A. Huse, Phys. Rev. B **38**, 386 (1988).
[32] D. S. Fisher and D. A. Huse, Phys. Rev. B **43**, 10728 (1991).
[33] S. Kirkpatrick and D. Sherrington, Phys. Rev. B **17**, 4384 (1978).
[34] H. Takayama and K. Hukushima, J. Phys. Soc. Jpn. **71**, 3003 (2002).
[35] H. Yoshino, A. Lematire, and J.-P. Bouchaud, Eur. Phys. J. B **20**, 367 (2001).
[36] P. E. Jönsson, R. Mathieu, P. Nordblad, H. Yoshino, H. Aruga Katori, and A. Ito, Phys. Rev. B **70**, 174402 (2004).
[37] P. E. Jönsson, H. Yoshino, and P. Nordblad, Phys. Rev. Lett. **89**, 097201 (2002).
[38] K. Fukao, A. Sakamoto, Y. Kubota, and Y. Saruyama J. Non-Cryst. Solids (to be published).